and E_c used in the calculation are given in Table I. To estimate the value of χ_0 we have used the barrier height[10] $\varphi = 3.6$ eV. In view of the simplicity of the model and the uncertainty in the experimental parameters, the agreement between theory and experiment for the quantity $\mathcal{S}_0$ is considered satisfactory (the uncertainty in the composition alone can account for the discrepancy). On the other hand, the theoretical value for the pre-exponential factor σ_0 exceeds the experimental one by a factor 30–100. Such a discrepancy is not surprising since σ_0 is very sensitive to the assumed shape and size of the grains and barriers and to the value of χ_0. The actual irregular shape of the grains could result in a substantially lower value of A than that corresponding to spherical grains. Also a variation in the value of d by a factor of 2 results in a factor of 30 for σ_0. The effects of finite energy-level separation, which for an irregular shaped 50-Å nickel grain is of the order of $E_F/nG \sim 1$ meV $\ll E_c$, have been neglected in view of the energy smearing introduced by the fluctuations in the charging energy. Such fluctuations are expected to result from electron-hole interactions. The temperature dependence of the conductivity, together with other related results, will be reported elsewhere.

We wish to thank Y. Arie for his technical assistance, M. Abrahams for making available to us the structural data on the Ni-SiO_2 system prior to publication, J. Hanak for providing the compositional analysis, and M. A. Lampert, A. Rothwarf, and J. D. Dow for valuable discussions. We are particularly indebted to A. Rose for the many illuminating discussions and suggestions.

*Present address: Institute for Advanced Study, Princeton, N. J. 08540.

[1]Interesting superconducting and ferromagnetic properties have also been observed in granular metals; e.g., B. Abeles and J. J. Hanak, Phys. Lett. 34A, 165 (1971), Y. Goldstein and J. I. Gittleman, Solid State Commun. 9, 1197 (1971).

[2]C. A. Neugebauer and M. B. Webb, J. Appl. Phys. 33, 74 (1962); C. A. Neugebauer, Thin Solid Films 6, 443 (1970).

[3]R. M. Hill, Proc. Roy. Soc., Ser. A 309, 377 (1969).

[4]N. C. Miller, B. Hardiman, and G. A. Shirn, J. Appl. Phys. 41, 1850 (1970).

[5]J. J. Hanak *et al.*, J. Mater. Sci. 5, 964 (1970).

[6]M. S. Abrahams, C. J. Buiocchi, M. Rayl, and P. J. Wojtowicz, to be published.

[7]L. Schiff, *Quantum Mechanics* (McGraw Hill, New York, 1968), 3d ed., p. 278.

[8]I. A. Campbell, Phys. Rev. Lett. 24, 269 (1970).

[9]The electron spends too short a time in the oxide for the low-frequency dielectric constant, $\epsilon = 4.2$, to be a valid parameter for describing the polarization of the oxide. See A. M. Goodman, Phys. Rev. 144, 588 (1966).

[10]Obtained as the difference between the work function of nickel, 4.6 eV [C. Kittel, *Introduction to Solid State Physics* (Wiley, New York, 1966), 3rd ed., p. 247] and the electron affinity of SiO_2, 1 eV [R. Williams, Phys. Rev. 140A, 569 (1965)]. Image-force lowering of the barrier has been neglected.

Effects of Electron-Plasmon Coupling on the Magneto-Optical Properties of Semiconductors

B. D. McCombe, R. J. Wagner, and S. Teitler
Naval Research Laboratory, Washington, D. C. 20390

and

J. J. Quinn*†
Brown University, Providence, Rhode Island 02912, and Naval Research Laboratory, Washington, D. C. 20390

(Received 7 September 1971)

Magnetotransmission experiments have been carried out on InSb samples ($4\times10^{14} < N < 6\times10^{16}$ cm^{-3}). These experiments reveal new absorption lines which are interpreted in terms of electron-plasmon interaction. Results are compared with a theoretical calculation.

In this Letter we report the first unambiguous observation of resonance absorption of infrared radiation due to plasmon-assisted electronic transitions in degenerate InSb in a magnetic field. To our knowledge this represents the first clear evidence of an absorption process which depends upon the interaction between individual conduction electrons and plasmons in semiconductors.

Electron-plasmon coupling in solids has been discussed by many authors since the pioneering

work on the subject by Bohm and Pines.[1] Similarities between the electron-plasmon interaction and the interaction between electrons and LO phonons[2] responsible for polaron effects in polar materials were emphasized by Lundqvist.[3] A number of effects of the electron-plasmon interaction were predicted, and the term "plasmaron"[4] was introduced to describe an excitation consisting of a plasmon coupled to a hole. The similarity between the polaron and electron-plasmon interactions led Teitler, McCombe, and Wagner[5] to extend the name plasmaron to the interaction between single-particle excitations and collective modes, and to look for "plasmaron" effects in the magneto-optical properties of degenerate semiconductors. The present work is an outgrowth of these ideas.

Magnetotransmission measurements were made on several samples of InSb having excess donor concentrations between 4×10^{14} and 6×10^{16} cm^{-3} at 77°K. A dual-beam pulsed molecular-gas laser ($H_2O/D_2O/SO_2$) system was used to provide a highly monochromatic source of far-infrared (IR) radiation,[6] and a Nb-Sn superconducting magnet system provided swept fields up to 95 kG. Samples were mounted in the Faraday or longitudinal geometry. The sample mounting and light-pipe system have been described elsewhere.[6] Laser frequencies were chosen such that $\omega_p<\omega<\omega_{LO}$, where $\omega_p=4\pi Ne^2/m^*\epsilon_0$ is the zero-field free-electron plasma frequency, and ω_{LO} is the LO phonon frequency.

A typical trace is shown in Fig. 1 for a sample having $N=2.2\times10^{15}$ cm^{-3} at 4.5°K. The left-hand side of the figure corresponds to the cyclotron-resonance-inactive (CRI) polarization while the right-hand side of the figure corresponds to the cyclotron-resonance-active (CRA) polarization. Circular polarizers (providing approximately 90% of the desired polarization) were fabricated from linear polarizers and quartz quarter-wave plates.[7]

We focus our attention on the transmission minimum indicated by the solid arrow 1 in the CRI polarization centered at ≈12 kG. We shall also mention briefly the weaker minima at 6 and 4 kG indicated by 2 and 3, respectively. The strong broad absorption in the CRA polarization results from overabsorbed cyclotron resonance in this thick sample ($d\approx4$ mm); and the monotonically increasing background in the CRI polarization is primarily due to the "wing" of this cyclotron resonance absorption. The CRI absorption line is weakly replicated in the CRA polarization as

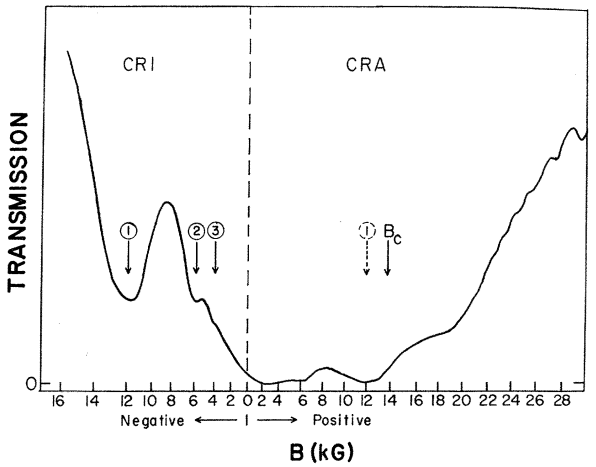

FIG. 1. Transmission versus magnetic field for a 4-mm-thick InSb sample with $N=2.2\times10^{15}$ cm^{-3} at 4.5°K and a laser frequency of 86.7 cm^{-1}. The magnetic field position of the free-electron cyclotron resonance as determined from a separate measurement on a thin sample of InSb ($N=7\times10^{13}$ cm^{-5}) is indicated by the arrow labeled B_c. The apparent asymmetry of the overabsorbed cyclotron resonance line results from low-field absorption due to the "harmonics," and the low-field analog of the process we describe in the text, i.e., plasmon-assisted free-carrier absorption.

a result of the imperfect polarizers (indicated by the dashed arrow 1).

This line was observed to move to higher fields as the laser frequency was increased. As carrier concentration was increased the line moved to lower fields at a given laser frequency. The variation of the position of this line for three different carrier concentrations is shown in Fig. 2. We also made a study of Voigt-shifted cyclotron resonance [which occurs at $\omega=(\omega_c^2+\omega_p^2)^{1/2}$] in two thin samples cut from the original thick samples having $N=2.2\times10^{15}$ and 6.3×10^{15} cm^{-3}. The CRI polarized line is close to, but at a resolvable distance below, this latter classical line position. Weak CRI lines may occur for any second-order optical transition in which single-particle Landau oscillator states are coupled by some interaction (e.g., electron–optical phonon); however, the movement of the observed CRI line with carrier concentration and magnetic field indicates that the interaction responsible for the line in this experiment is the electron-plasmon interaction. Data from the two lowest concentration samples are not plotted on this figure because of complications from impurity shifted cyclotron resonance.

Satellite "lines" on either side of the cyclotron resonance have been observed in a variety of

semiconducting materials.[8] Although a number of theoretical explanations have been proposed, the most recent model consists of a combination of multiple-reflection and Faraday-rotation interference effects.[9] The importance of such effects was pointed out previously by the present authors.[10] These effects are excluded in this experiment since the position of the CRI line was unaffected by severe wedging, roughening, or thinning of the sample.

The process we believe responsible for the CRI resonance absorption was previously suggested in Ref. 5. It is discussed in the following theoretical treatment and is justified by comparison of the results of this calculation with the experiments.

We shall treat the conduction electrons in InSb as free electrons of effective mass m^* moving in a medium of dielectric constant ϵ_0. For wavelengths sufficiently short that $cq > \omega$, the longitudinal plasma modes are not strongly influenced by retardation effects, and the dispersion of these modes can be determined by simply setting the longitudinal dielectric constant $\epsilon_l(\omega)$ equal to zero. The roots of the resulting equation can be written[11]

$$\omega_\pm^2(\theta) = \tfrac{1}{2}(\omega_c^2 + \omega_p^2) \pm [\tfrac{1}{4}(\omega_c^2 + \omega_p^2)^2 - \omega_c^2\omega_p^2\cos^2\theta]^{1/2}. \quad (1)$$

In this equation θ is the angle between q (the plasmon wave vector) and the dc magnetic field, and ω_c is the cyclotron frequency. We shall use the root ω_+ of Eq. (1) to describe the magnetoplasma modes observed in the present experiment.[12]

The interaction between the electrons and plasmons can be written[3,5]

$$H_{e,\mathrm{pl}} = \textstyle\sum_{\vec{q}}{}' D(\vec{q}) e^{i\vec{q}\cdot\vec{r}} (b_{-\vec{q}} + b_{\vec{q}}^{+}), \quad (2)$$

where b_q annihilates a plasmon of wave vector q and

$$D(q) = \left[\frac{4\pi e^2\hbar}{q^2\Omega(\partial\epsilon_l/\partial\omega)_{\omega_+}}\right]^{1/2}.$$

The sum over q in Eq. (2) should be restricted to values for which the plasmon is well defined. In the absence of a dc magnetic field this restriction is $|\vec{q}| < q_c$, and the cutoff wave number q_c is simply that value of q at which $\omega_p(q)$ intersects the particle-hole continuum.[13] The general question of plasmon lifetime in the presence of a dc magnetic field is much more complicated.[14]

We assume that $\omega_c \gg \omega_p$ and only the lowest Landau level is occupied, conditions which generally describe the experimental situation. The ω_+ plasmons described by Eq. (1) are stable if $q_z < k_F[(1+\beta)^{1/2} - 1]$, where $\beta \simeq \hbar\omega_p^2/\omega_c\epsilon_F$, $\epsilon_F = \hbar^2 k_F^2/2m^*$ being the Fermi energy measured from the bottom of the lowest Landau level. Thus, we restrict the summation appearing in Eq. (2) to values of $\vec{q}$ for which $q_z < k_F[(1+\beta)^{1/2} - 1]$.

The electronic states in the presence of the dc magnetic field are described by eigenfunctions $|\nu\rangle = |n, k_y, k_z\rangle$, where n is the Landau quantum number. In the second-order process responsible for the CRI resonance absorption, the first step is virtual electron-hole pair creation accompanied by plasmon emission resulting from the electron-plasmon interaction. In this step the initial electron in the state $|n=0, k_y, k_z\rangle$ emits an $\omega_+(-\vec{q})$ plasmon and jumps to an intermediate state $|n=1, k_y+q_y, k_z+q_z\rangle$. The photon absorption, which is the second step, results from the electron-photon interaction, $(e/c)\vec{v}\cdot\vec{A}$, where $\vec{v}$ is the electron velocity and $\vec{A}$ is the vector potential of the photon field. In order to make the transition from the $|n=1, k_y+q_y, k_z+q_z\rangle$ state to the $|n=0, k_y+q_y, k_z+q_z\rangle$ final state, CRI radiation is

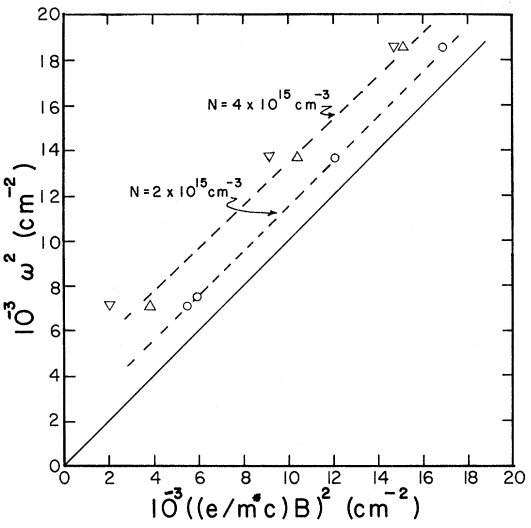

FIG. 2. Laser frequency squared versus the square of the magnetic field position of the various absorption lines. On this plot, cyclotron resonance appears as a straight line through the origin of slope 1 (solid line). The CRI absorption line (1 from Fig. 1) for several laser frequencies is plotted for three different carrier concentrations: inverted triangles, $N = 6\times10^{16}$ cm^{-3}; triangles, $N = 6.3\times10^{15}$ cm^{-3}; circles, $N = 2.2\times10^{15}$ cm^{-3}. Theoretical calculations (see text) for two sample concentrations are shown as the dashed lines.

absorbed. The transition rate and the power absorbed by this process can be calculated by Fermi's "golden rule." The rate of scattering from initial state i to final state f is

$$w_{fi} = (2\pi/\hbar)|M_{fi}|^2\delta(E_f - E_i). \tag{3}$$

For the process described above M_{fi} is given by

$$M_{fi} = \langle\nu''\left|\frac{e}{c}\vec{v}\cdot\vec{A}\right|\nu'\rangle\langle\nu'|\textstyle\sum_q' D(\vec{q})e^{i\vec{q}\cdot\vec{r}}|\nu\rangle/[E_\nu - E_{\nu'} - \hbar\omega_+]. \tag{4}$$

The power absorbed is obtained by multiplying Eq. (3) by the photon energy $\hbar\omega$ and summing over initial and final states. The matrix elements appearing in Eq. (4) can be easily evaluated.[15] The resulting expression for the power absorbed per unit volume is

$$P = \frac{m^*e^4\omega^2}{4\pi^2\hbar^3c^2\epsilon_0}|A|^2\left[\frac{t^2}{(1+t)^2}\int_0^{\pi/2}d\theta\tan\theta\,\frac{\Omega_+(\Omega_+^2 - t^2)}{\Omega_+^2 - \Omega_-^2}\int' dx\,e^{-x}\right]. \tag{5}$$

Here $t = \omega_c/\omega$ and $\Omega_\pm = \omega_\pm/\omega$. The parameter $x = \hbar q_\perp^2/2m^*\omega_c$, and limits on the x integration are determined by the exclusion principle and the requirement that $q_z < k_f[(1+\beta)^{1/2} - 1]$. The part of Eq. (5) within the bracket is a function of the parameter t; this function $F(t)$ has been evaluated numerically for several different frequencies and electron concentrations. For low concentrations, $F(t)$ is rather sharply peaked with noticeable asymmetric broadening to the low-field side. For higher concentrations the functions are broader and quite symmetric.

In addition to the fundamental absorption described above, "harmonics" occur when the initial plasmon emission is accompanied by an electronic transition from the $n = 0$ to $n = \alpha + 1$ state. The resonance frequency for these transitions is shifted approximately $\alpha\omega_c$ from the fundamental. The lines in Fig. 1 indicated by 2 and 3 occur at slightly *lower* fields than exact harmonics of cyclotron resonance. Similar lines have been attributed to harmonics of cyclotron resonance by other workers,[16] although a satisfactory explanation for these relatively intense lines has not been given. We suggest that the electron-plasmon mechansim described above may be the appropriate explanation.

The peak positions obtained from the numerical calculations of $F(t)$ for the two indicated carrier concentrations are shown in Fig. 2 as the two dashed lines. We note that the theoretical curve and experimental points for $N = 2\times10^{15}$ cm^{-3} are in excellent agreement. The data for $N = 6.3\times10^{15}$ and 6×10^{16} cm^{-3} samples are shifted in the direction indicated by the calculation for $N = 4\times10^{15}$ cm^{-3}. This latter concentration represents the highest concentration for which population of higher Landau levels may be neglected at the lowest operating frequency. It seems likely that the positions of the lowest-frequency experimental points for $N = 6.3\times10^{15}$ and certainly for $N = 6\times10^{16}$ are shifted to higher magnetic fields because of population of higher Landau levels and nonparabolicity.

An intuitive understanding of the position of the peaks can be obtained by noting that the dominant contribution to the absorption comes from plasmons with q nearly perpendicular to $\vec{B}$ so that $\omega_+ \simeq (\omega_p^2 + \omega_c^2)^{1/2}$. Furthermore, the average energy of the excited electron-hole pair can be shown to be of the order of the Fermi energy, $\epsilon_F = \hbar\omega_F$ ($\epsilon_F \propto B^{-2}$). Thus, the resonance frequency should be of the order of $(\omega_c^2 + \omega_p^2)^{1/2} + \omega_F$, in qualitative agreement with experiment and the numerical calculation. A comparison of the experimental and calculated peak absorption strengths shows that the experimental strength is roughly 4 times larger than the theoretical estimate. We consider this reasonable agreement considering the simplifying assumptions involved in the calculation and the difficulty in extracting accurate experimental estimates of the line intensity.

More detailed experiments and calculations including studies of the "harmonics" will be presented in subsequent publications.

Note added in proof.—After this Letter was submitted, a Letter by Shay *et al.* [J. L. Shay, W. D. Johnson, Jr., E. Buehler, and J. H. Wernick, Phys. Rev. Lett. 27, 711 (1971)] appeared with a claim to have observed plasmaron coupling in $CdSnP_2$. However, they did not provide a quantitative analysis of their data. At present, we do not understand how their data can be explained in terms of plasmaron coupling.

The authors are grateful to Dr. G. A. Prinz for valuable contributions concerning the design of efficient far-IR polarizers, to Mr. P. G. Siebenmann for making the transport measurements,

to Mr. K. W. Chiu for performing the numerical calculations, and to Dr. K. L. Ngai and Professor E. Burstein for helpful discussions.

*Permanent address: Brown University, Providence, R. I. 02912.

†Work supported in part by the National Science Foundation and the Advanced Research Projects Agency.

[1]D. Bohm and D. Pines, Phys. Rev. 92, 609 (1953).

[2]H. Fröhlich, Advan. Phys. 3, 325 (1954).

[3]B. I. Lundqvist, Kgl. Dan. Vidensk. Selsk., Mat.-Fys. Medd. 6, 193 (1967).

[4]L. Hedin, B. I. Lundqvist, and S. Lundqvist, *Electronic Density of States*, National Bureau of Standards Special Publication No. 323 (U. S. GPO, Washington, D. C., 1970).

[5]S. Teitler, B. D. McCombe, and R. J. Wagner, in *Proceedings of the Tenth International Conference on the Physics of Semiconductors*, edited by S. P. Keller, J. C. Hensel, and F. Stern, CONF-700801 (U. S. AEC Division of Technical Information, Springfield, Va., 1970), p. 177.

[6]R. J. Wagner and G. A. Prinz, Appl. Opt. 10, 2060 (1971).

[7]G. A. Prinz, R. J. Wagner, and B. D. McCombe, to be published.

[8]The initial observation in CdS was reported by K. J. Button, B. Lax, and D. R. Cohn, Phys. Rev. Lett. 24, 375 (1970). For a more complete bibliography concerning other materials, see T. L. Cronburg and B. Lax, Phys. Lett. 37A, 135 (1971).

[9]Cronburg and Lax, Ref. 8.

[10]B. D. McCombe, R. J. Wagner, and G. A. Prinz, Bull. Amer. Phys. Soc. 15, 364 (1970).

[11]See, for example, V. Celli and N. D. Mermin, Ann. Phys. (New York) 30, 249 (1964).

[12]This assumption is consistent with our result that the plasmons which make the dominant contribution to the observed resonance absorption satisfy the condition $cq > \omega$.

[13]J. J. Quinn and R. A. Ferrell, Bull. Amer. Phys. Soc. 1, 144 (1956).

[14]See, for example, N. J. Horing, Ann. Phys. (New York) 31, 1 (1965).

[15]See, for example, J. J. Quinn and S. Rodriguez, Phys. Rev. 128, 2487 (1962).

[16]See, for example, E. J. Johnson and D. H. Dickey, Phys. Rev. B 1, 2676 (1970).

Observation of $T = 23$ Double Analog States in ^{210}Po†

G. W. Hoffmann, G. J. Igo, C. A. Whitten, Jr., W. H. Dunlop, and J. G. Kulleck
Department of Physics, University of California, Los Angeles, California 90024
(Received 26 August 1971)

The T 23 states in $^{210}_{84}Po_{126}$ ($T_3 = 21$) which are the isobaric analogs of the $T = T_3 = 23$ ground state and low-lying states in $^{210}_{82}Pb_{128}$ have been observed as enhancements in the excitation function for the reaction $p + {}^{209}_{83}Bi_{126} \rightarrow {}^{208}_{82}Pb_{126} + 2p$. The experimentally observed enhancements in the two-proton coincidence excitation function correlate with the known level structure of ^{210}Pb and occur at the incident proton energies predicted by Coulomb energy formulas, thus establishing that these enhancements are due to the population of double analog levels in ^{210}Po.

For the neutron-rich, heavy nuclei [$T_3 = (N - Z)/2 \gtrsim 10$] the experimental observation of double analog states — states with isospin T greater by 2 than T_3 — has not been previously reported. In lighter nuclei such states have been strongly excited by direct reactions such as the (p, t) reaction.[1] However, in the (p, t) reaction the $T = T_3 + 2$ states are excited by a factor approximately proportional to $1/T^2$ compared with the $T = T_3$ states in the same nucleus.[2] For nuclei around ^{208}Pb $T \simeq 22$, so that the excitation of double analog states by direct reactions such as (p, t) is greatly inhibited.

In the present experiment the $T = 23$ double analog states in $^{210}_{84}Po_{126}$ are reached via the entrance channel $p + {}^{209}_{83}Bi_{126}$ ground state. Since the isospin of the ^{209}Bi ground state is only $\frac{43}{2}$, the entrance channel has a maximum isospin of $T = 22$; and thus the $T = 23$ states in ^{210}Po can only be reached via isospin mixing due to the isospin-nonconserving parts of the Coulomb force. In turn, this means that the cross section for the formation of double analog states in ^{210}Po via the $p + {}^{209}$Bi entrance channel is expected to be very small. For the incident proton energies at which the double analog states are excited ($E_{p\,\mathrm{in}} \simeq 33$ MeV) the total reaction cross section is approximately 2 b. Thus, the observation of the double analog states depends on the existence of a very unique signature for their decay.